Transactions, SMiRT-24
BEXCO, Busan, Korea - August 20-25, 2017
Division VI
Paper ID: 06-07-02

INVESTIGATION OF ACCIDENT THERMAL EFFECTS ON REINFORCED CONCRETE BEAMS

Amit H. Varma[1], Kadir C. Sener[2] and Saahastaranshu R. Bhardwaj[3]

[1] Professor, Lyles School of Civil Engineering, Purdue University, West Lafayette, IN, USA
[2] Research Engineer, Lyles School of Civil Engineering, Purdue University, West Lafayette, IN, USA
[2] Ph.D. Student, Lyles School of Civil Engineering, Purdue University, West Lafayette, IN, USA

ABSTRACT

Safety-related reinforced concrete (RC) structures have to be designed for mechanical & thermal loading resulting from accident scenarios such as high-energy pipe break. Experimental tests have been performed in order to evaluate the effects of mechanical + accident thermal loading on the out-of-plane flexural and shear behavior of reinforced concrete (RC) walls.

This paper summarizes and compares the experimental findings obtained from full scale RC beam specimens that were subjected to different combinations of thermal heating and out of plane mechanical loading. The experimental program consisted of three full-scale RC beam tests that were subjected to four point-load bending. The test matrix included one control specimen at ambient condition and two specimens with heating on one of the shear spans. The specimens were subjected to an idealized heating condition by maintaining constant surface temperature for three hours before loading to failure. The principal parameter included in the experimental investigations; was the maximum accident temperature.

The experimental results indicate that accident thermal conditions have influenced the out-of-plane shear strength of the tested RC beams depending on the maximum surface temperature. The experimental results included measured fundamental responses such as; shear force-mid-span displacement, shear force-shear strain, and temperature gradients through beam cross-sections. These experimentally obtained responses were utilized for discussions regarding the out-of-plane flexural and shear stiffnesses, and shear strength of the tested specimens. The measured shear strengths obtained from the tests were also compared with American code provisions to verify their applicability to RC beams at elevated temperatures.

INTRODUCTION

The objective of the combined accident thermal and mechanical loading tests was to experimentally investigate the out-of-plane flexural and shear behavior of a typical reinforced concrete (RC) element subjected to nonlinear thermal gradients. An additional objective was to investigate the applicability and conservatism of design shear strength equations developed for ambient conditions to RC members subjected to combined thermal and mechanical loading.

Reinforced concrete walls in nuclear power plant constructions require high (1-2%) reinforcement ratios in order to provide adequate design strength to meet the design (force and moment) demands. Therefore, these walls typically include large diameter vertical and horizontal reinforcement rebars (#11 or larger) at small spacing. These walls also include ties or hoops as means of out-of-plane shear reinforcement to meet the out-of-plane shear demands. This experimental research consists of testing beams that represent one-way beam strips taken from reinforced concrete walls of nuclear facilities. The reinforced concrete beams that were tested as part of this research were designed to fail in flexural-shear failure mode, which corresponds to the lower bound shear strength. The desired failure mode was achieved by optimizing the longitudinal and shear reinforcement, and shear-span-to-depth (a/d) ratios; so that the out-of-plane flexural

strength is slightly greater than the out-of-plane shear strength of the tested beams. Strength results from prior testing of similar reinforced concrete beams were utilized to accurately estimate the experimental shear strength, e.g. (Yang et al., 2015).

As discussed in Booth et al. (2016), accident thermal loading typically subjects the walls to heating on both sides of the compartment. The first few hours of the heating results in nonlinear thermal gradient through the cross-section because of the large thermal mass and low conductivity of concrete. These nonlinear temperature profiles and different thermal properties of steel and concrete result in cracking in concrete which may cause reduction in stiffness and strength of reinforced concrete members.

EXPERIMENTAL SETUP

Test Matrix

An experimental study was conducted with a test matrix consisting of three specimens. The summary of the test matrix and relevant geometric details of the specimens are given in Table 1. RB-A- was the control specimen which was tested at ambient conditions. RB-300 was heated with a surface temperature of 300°F for 3 hours on both top and bottom surfaces in the one of the shear spans. RB-450 was tested using the same procedure as for RB-300, the only difference being the target surface temperature of the specimen was 450°F.

Table 1 – Test matrix

Specimen ID	Beam thick. (T)	Rebar size & quantity	Reinf. ratio %	Stirrup spacing (S)	Clear cover (in.)	Max. temp.	Heating duration	Parameter
RB-A	24 in.	4-#11	1.83%	2#4@10.5 in	1.5 in.	Amb.	-NA-	Control Specimen
RB-300	24 in.	4-#11	1.83%	2#4@10.5 in	1.5 in.	300°F	3 hours	Effect of Heating
RB-450	24 in.	4-#11	1.83%	2#4@10.5 in	1.5 in.	450°F	3 hours	Max. Temperature

Specimen details

The shear span-to-height ratio (a/h) of all the specimens was set equal to 2.5. The three beam specimens tested as part of this research were identical. All the specimens had a clear cover of 1.5 in. Each of the specimens had a thickness of 24in., width of 16in., and doubly reinforced with four #11 bars each at the top and bottom, that is equal to a longitudinal reinforcement ratio of 1.83% ($A_s/b_w d$). #4 hoops at 10.5 in. spacing served as the shear reinforcement, where the spacing was set equal to half of the effective depth of section ($d/2$). The geometric dimensions with load and heating locations, and reinforcement details of the specimens used for this study are shown in Figures 1 and 2.

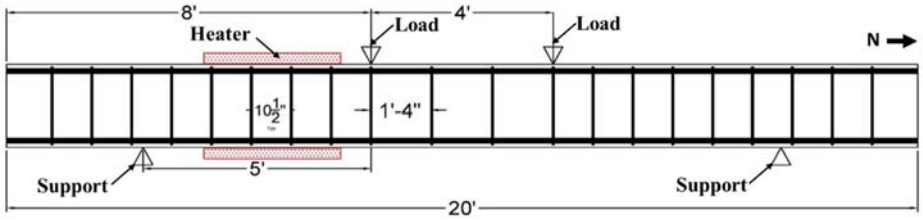

Figure 1 - Beam Geometry with Loading and Heating Regions

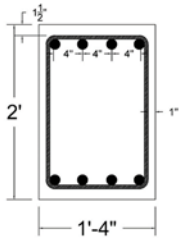

Figure 2 - Specimen cross-sections with reinforcement details

Test setup

The accident thermal test specimens were subjected to four-point bending with two concentrated loads and simply supported ends. The concentrated loads were applied symmetrically about the center of the specimen. The tests were conducted by subjecting each specimen to a combination of heating and monotonically increasing loading at the two load points. Heaters were placed on opposing surfaces on the south side of the specimen to apply the thermal loading as shown in Figure 1. The out-of-plane loading was applied to the beam specimens using load spreader beams. The specimen ends were supported using cylindrical bearings that permit rotation and sliding (translation) at the supports as needed. This accident thermal test setup has been previously utilized by the authors (Booth et al. 2016) for evaluating the effects of accident thermal loading on the behavior of steel-concrete composite (SC) beams.

An isometric view of the test setup including the heaters and mechanical load frame is shown in Figure 3. Insulating materials were provided between the specimen surface and heaters to minimize heat loss. The north side of the specimen was maintained at ambient condition. The applied temperatures were controlled using thermocouples attached to the surfaces of the reinforced concrete beams. The exposed surface time-temperature curve was controlled by the thermal controller and data acquisition system, which was independent of the remaining thermocouples and data acquisition instrumentation system.

Loading Protocol

Thermal and mechanical loading were applied to each specimen in the order and magnitudes that are presented here:

Step 0. This step applies an out-of-plane shear force of 25 kips to the test specimen. This force is calculated based on half of the concrete design shear strength contribution in ACI 349 $\left(\sqrt{f'_c}\cdot b_w \cdot d\right)$, using a nominal concrete compressive strength of 4000psi.

Step 1. This step applies thermal loading (heating) to the test specimen while maintaining the applied loading from Step 0. The applied loading is kept constant in order to represent the sustained loading in the wall during an accident. The specimen surfaces are heated to target temperatures given in Table 1 as rapidly as practical (20-30 minutes approximately) and the surface temperature is maintained for at least 3 hours at the target temperature.

Step 2. The applied out-of-plane loading is monotonically increased from the load level at the end of Step 1 (25 kips) to failure while maintaining the heating.

The time history of the thermal and mechanical loading protocol implemented in the testing of the heated specimens is illustrated in Figure 4. The plot is obtained from the experimental results of the specimen with surface heating of 300°F (RB-300).

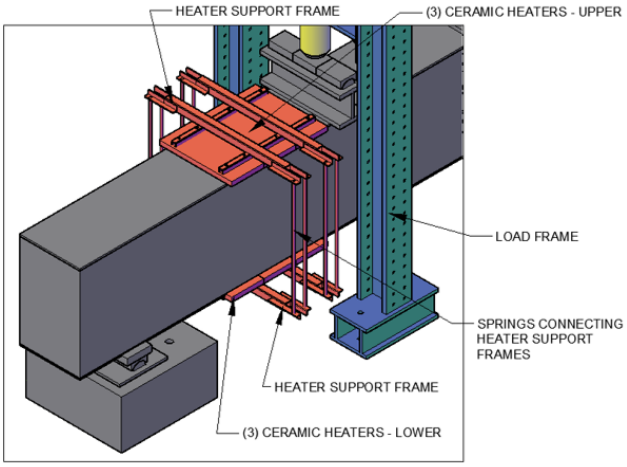

Figure 3 – Accident Thermal Test Setup

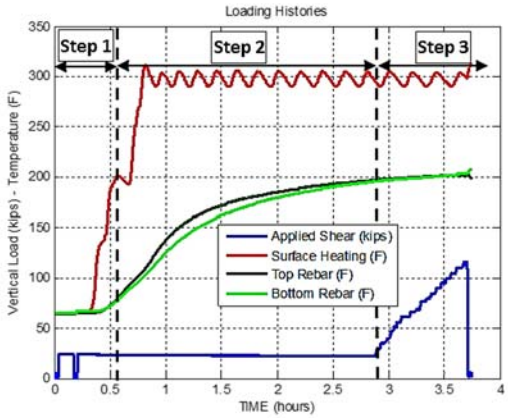

Figure 4 –Loading History and Rebar Temperatures of RB-300

Sensor Layout

The specimen response was measured using various sensors at several locations during each test. These instrumentation included displacement sensors, inclinometers, strain gauges and thermocouples. A common instrumentation layout was adopted for the specimens, and the details of the instrumentation placement are illustrated in Figures 5 and 6 and discussed below.

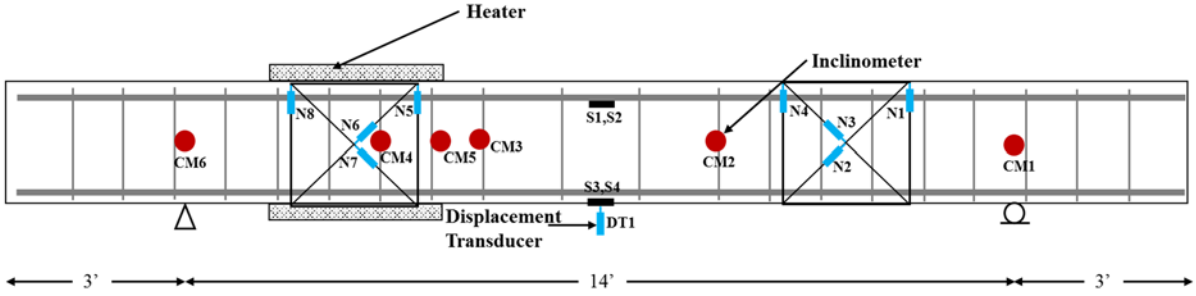

Figure 5 - Locations of sensors

1. Displacement sensors were placed at the mid-span of the specimen to measure vertical deflections as shown in Figure 5. Support settlements were also measured using displacement sensors to calculate the chord (net) vertical deflection. Additional displacement sensors were attached to the concrete face in order to monitor and measure the opening of the section due to concrete cracking.
2. Inclinometers were attached to the beam cross-sections at the load and support locations. Additional inclinometers were attached in the heated region to calculate the average flexural stiffness in that region.
3. Steel strain gauges were located on both longitudinal and shear reinforcements as shown in Figure 6. The strain gauges on the longitudinal reinforcement were placed in the constant moment region in between the load points. The strain gauges on vertical legs of the shear reinforcement (hoops) were placed at the mid-height of the cross-section in the heated shear span. These reinforcement strains were used to monitor, steel yielding, assess concrete cracking, and identify failure modes. Since the strain gauges were placed away from the heaters, standard strain gauges were used instead of high-temperature strain gauges.
4. Type K thermocouples were attached at various locations throughout the specimen in order to monitor the temperature during the tests. Type K thermocouples are capable of measuring temperatures in the range of -328° F to 2282°F (-200°C to 1250°C). These thermocouples were mounted on to the concrete surfaces, and welded to both the longitudinal and shear reinforcement bars. A rod consisting of a

threaded rod with thermocouples welded along the length, also referred as "thermocouple tree", was used to measure the temperature through the depth of the concrete. The rod was positioned prior to casting, and the rod and thermocouples were embedded in the concrete as shown in Figure 6.

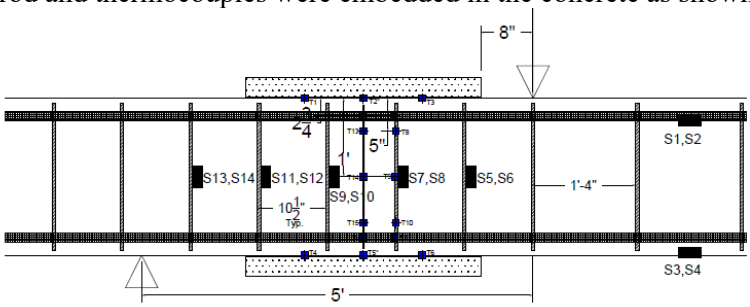

Figure 6 - Locations of Strain gauges and Thermocouples in the Heated Region

EXPERIMENTAL RESULTS

The results from the experimental program are presented in this section. The heated specimens exhibited similar behavior with slight differences at the ultimate force levels.

Specimen RB-A

This specimen was tested as a control specimen under ambient conditions to confirm and compare the effects of accident thermal and out-of-plane shear loading. It was subjected to out-of-plane loading only. The force-displacement response shown in Figure 7 indicates a nearly elastic response up to the peak load level and then a negative post-peak slope indicating the shear failure of the specimen. Some nonlinearity was observed in the ascending portion of the force-deflection response due to cracking of the concrete and yielding of the shear reinforcement rebars. In this figure, the average force is calculated by taking the average of the forces applied by the two hydraulic rams. The vertical deflections were obtained from the mid-span displacement measurements. The specimen reached its peak force at 129 kip load with 0.68 inches of mid-span displacement, where shear failure of the specimen occurred at this point as shown in Figure 8. The specimen lost its force capacity and was unloaded after significant reduction in the load carrying capacity. The horizontal lines in the figure indicate the nominal shear strength (V_n) and the concrete contribution to the nominal shear strength (V_c) calculated per ACI 349. As shown, the specimen shear strength is greater than that the design shear strength calculated using measured properties with about 23%.

Figure 9 shows the variation in shear reinforcement strain for the final two loading cycles. The shear reinforcement strains were obtained from the hoops that are approximately 2 feet south of the mid-span section. This region corresponds to the heated-region in the heated specimens. The initiation of strain readings in the shear reinforcement hoops was observed at around 50 kips. The yield strain was calculated as 2348 micro strain based on the measured yield strength of the shear reinforcement rebars (f_{y_hoop} = 68.1 ksi). This yield strain was reached at about 100 kips and the strain increased with the applied loading until the failure. The shear reinforcement strains were well beyond yielding and the longitudinal reinforcement strains were within elastic range during the failure, which confirms the failure mode as shear and not flexural yielding. The shear failure was due to extensive yielding in the shear reinforcement which resulted in dense and wide diagonal cracks and failure in concrete as seen in the failure picture in Figure 8.

Figure 10 shows the shear force vs. shear strain response calculated from diagonally placed displacement sensors located in the shear spans of the specimen. The deformations along the diagonal were utilized to calculate the average shear strain in the region. The slope of the shear force-shear strain curve was calculated to obtain the shear stiffness and compared with the heated specimen in the latter sections.

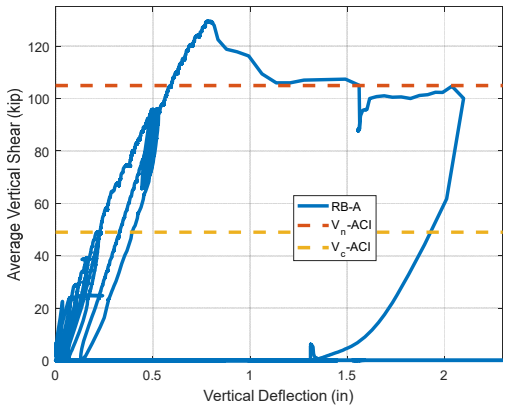

Figure 7 – Average shear force vs. mid-span displacement

Figure 8 - Diagonal Shear Failure in the Shear Span (East Face)

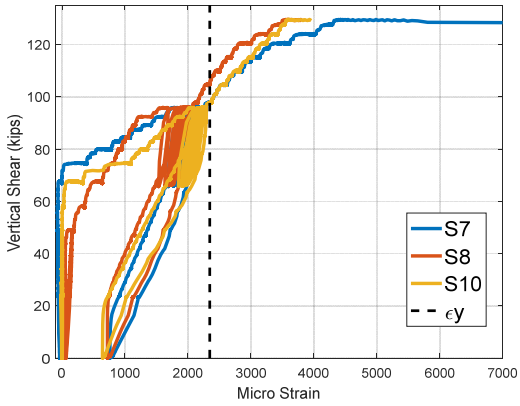

Figure 9 – Average shear force vs. shear reinforcement strains

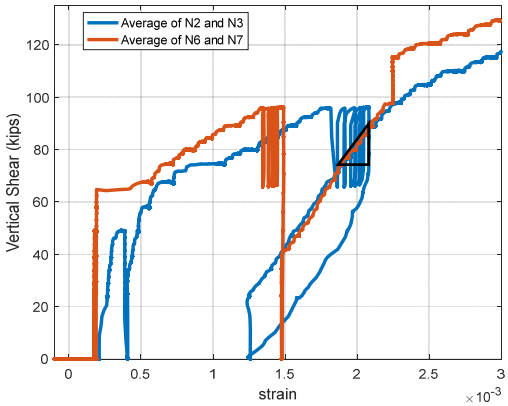

Figure 10 – Average shear force vs. average shear strain

Specimen RB-300

This specimen was heated to 300°F on both top and bottom surfaces on the south shear span to investigate the effects of accident thermal loading on the out-of-plane behavior. The specimen experienced through-depth cracks in the heated zone (south shear span) after reaching the target surface temperature (Step 1), following the initial loading of 24 kips (Step 0). These cracks in the shear span were observed at higher force levels for the ambient specimen. The early occurrence of these cracks in the shear span have resulted in wider crack widths than the ambient specimen at similar load levels, as discussed in the latter sections.

The average shear force vs. mid-span displacement response of the heated specimen is compared with the ambient specimen in Figure 11. The heated specimen reached its peak load at 116 kips with 0.75 inches of mid-span displacement. Shear failure of the specimen occurred at this point, and the specimen started losing its load carrying capacity from this point onwards. Comparison with the ambient specimen indicates that the combination of applied thermal and mechanical load has resulted in reductions in both stiffness and strength of the specimen. The shear strength of this heated specimen was larger than the nominal shear strength calculated per ACI 349 (V_{exp}=116 kips vs. V_n=105 kips), despite the strength reduction due to heating.

Figure 12 illustrates the evolution of thermal gradient through the section depth during the heating duration. The thermal gradients are obtained from the thermocouple measurements attached to a shear reinforcement bar. The plot is symmetric between top and bottom temperature measurements indicating that the heaters were functional on the top and bottom surfaces. Thermally induced cracking occurred almost immediately after the onset of heating. These cracks were caused by differential thermal expansion of the steel and concrete resulting from the vertical temperature gradient extending through the section depth.

Thermally induced cracking during the heating phase resulted in shear reinforcement strains at a lower force levels than the ambient specimen (25 kips vs. 50 kips). The shear reinforcement bars also reached the yield strain level at a lower force than the ambient specimen (60 kips vs. 100 kips), which eventually caused the softer response and reduction in the shear strength.

The shear force vs. shear strain response obtained from both shear spans (heated & unheated) are shown in Figure 14. Consistent with the load-displacement response comparisons between the ambient and heated specimens, a lower shear stiffness was observed for the heated shear span (south) compared to the ambient shear span (north) of specimen RB-300.

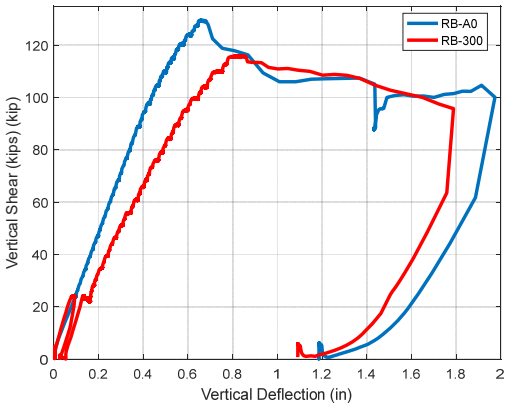

Figure 11 – Average load vs. mid-span displacement

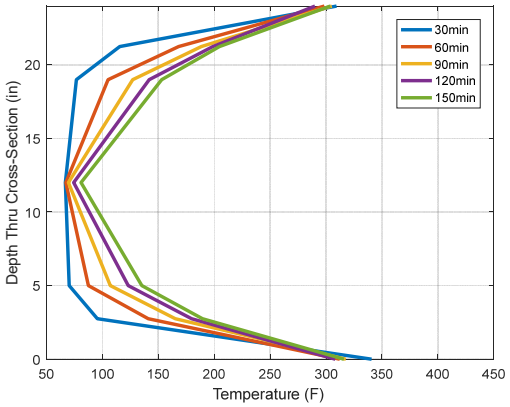

Figure 12 – Through-depth temperature distribution

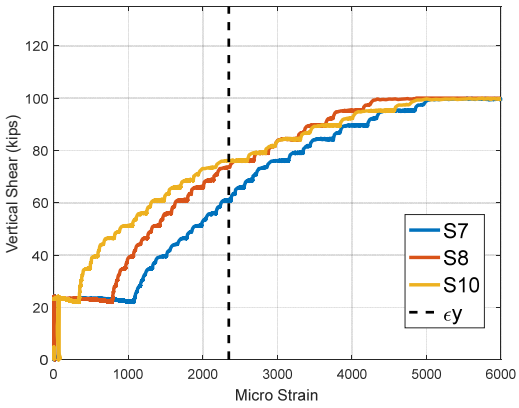

Figure 13 – Average shear force vs. shear reinforcement strains

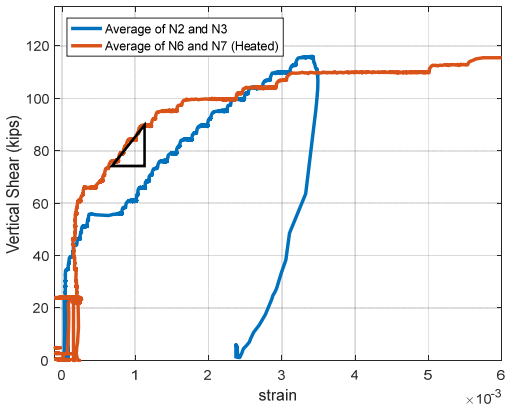

Figure 14 – Average shear force vs. average shear strain

Specimen RB-450

This specimen was heated to 450°F on both top and bottom surfaces on the south shear span to investigate the effects of higher surface temperature on the out-of-plane behavior. This specimen also experienced through-depth cracks in the heated zone (south shear span) after reaching the target surface temperature.

In Figure 15, the average shear force vs. mid-span displacement response of the specimen is compared with both the ambient specimen (RB-A) and the specimen heated to 300°F (RB-300). This specimen with surface target temperature of 450°F reached its peak load at 100 kips with 0.63 inches of mid-span displacement and underwent shear failure at this point. The strength comparison with RB-300 indicates that the increase in surface temperature resulted in further reduction in the shear capacity. The shear strength of RB-450 was slightly less than the nominal shear strength calculated according to ACI 349 (V_{exp}=100 kips vs. V_n=105 kips).

Figure 16 illustrates the evolution of thermal gradient through the concrete depth during the heating duration. The thermal gradient is obtained from thermocouple measurements attached to a tie bar. The plot is symmetric between top and bottom temperature measurements indicating the heaters were functional on the top and bottom plate.

Figure 17 shows that the shear reinforcements reached yield strain at about 60 kips, similar to RB-300. The shear force vs. shear strain response obtained from both shear spans (heated & unheated) are shown in Figure 18, with a lower shear stiffness observed in the heated shear span.

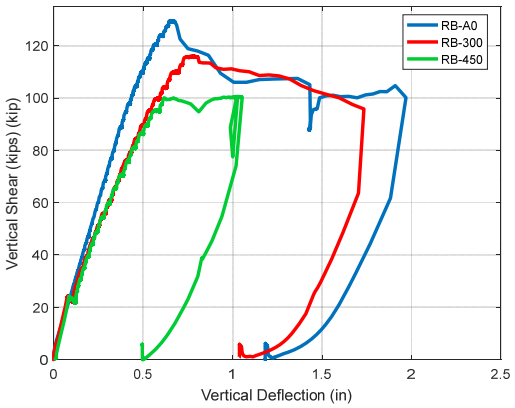

Figure 15 – Average load vs. mid-span displacement

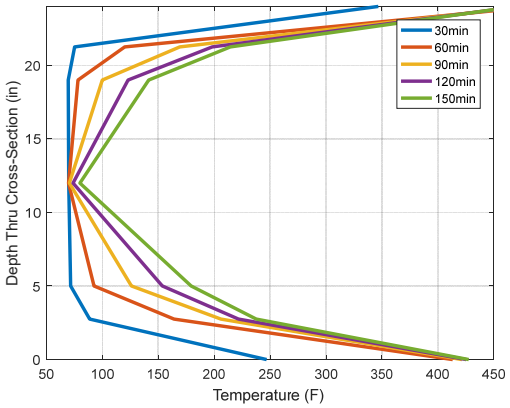

Figure 16 – Through-depth temperature distribution

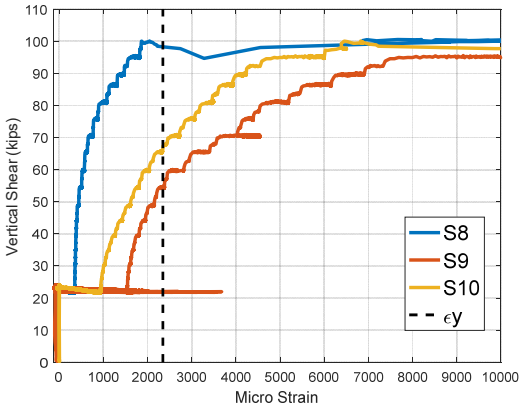

Figure 17 – Average shear force vs. shear reinforcement strains

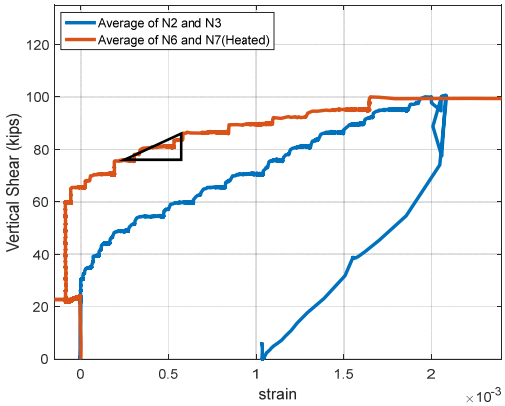

Figure 18 – Average shear force vs. average shear strain

SUMMARY OF EXPERIMENTAL RESULTS

The force-displacement curves for the three specimens tested as part of this research are shown in Figure 15. It is evident that thermal loads reduced the stiffness and strength of the specimens. The maximum load-carrying capacity (V_{exp}), as recorded in Table 2, was decreased with application of thermal load combinations. The code calculated strengths (V_n - ACI) were less than the experimentally measured strengths for the ambient (RB-A) and the specimen heated to 300°F (RB-300), but slightly greater for the specimen heated to 450°F (RB-450).

Figure 20 shows the crack widths measured during the testing of the specimens at different load levels. The figure indicates that the heated specimens exhibited wider crack widths than the ambient specimen. The crack widths increased with higher surface temperatures.

The shear stiffness of the specimens obtained from the slope of the shear force vs. shear strain curves at the shear force of about 80 kips are summarized in Table 3. The shear stiffness of the ambient specimen was measured to be 12% of the shear stiffness of the un-cracked concrete section (A_cG_c). The shear stiffnesses of the heated specimens were reduced further to less than 5% of the un-cracked concrete shear stiffness and about 30% of the ambient specimen shear stiffness.

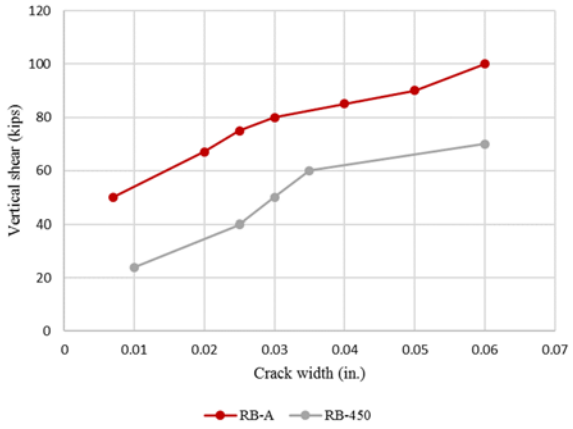

Figure 20 – Comparison between Shear Crack Widths at different loads

Table 2 – Comparison of Experimental and Code Calculated Strengths

Specimen ID	f'_c (ksi)	f_y (rebar)	f_y (hoop)	V_c(ACI) (kips)	V_n(ACI) (kips)	V_{exp} (kips)	$\frac{V_{exp}}{V_n}$
RB-A	5.265	71.1 ksi	68.1 ksi	49	105	129	1.23
RB-300						116	1.10
RB-450						100	0.95

Table 3 – Comparison of Specimen Shear Stiffness in the Heated Region

Specimen ID	Stiffness, k_{xy}	$k_{xy}/k_{xy(RB\text{-}A)}$	k_{xy}/G_cA_c
RB-A	77954.6	1.00	0.12
RB-300	26185.5	0.34	0.04
RB-450	23568.9	0.30	0.04

CONCLUSIONS AND FUTURE WORK

This paper presents the findings from an experimental testing program of three reinforced concrete beam specimens that were subjected to thermal heating and out-of-plane shear loading. The test matrix included one control specimen at ambient condition and two specimens with heating in one of the shear spans. The heated specimens had different maximum temperatures of 300°F and 450°F.

The measured shear strength for the ambient RC beam specimen was 23% higher than the code calculated strength. The experimental shear strength of the specimen heated to 300°F was reduced but was still larger than the code calculated strength by 10%. The shear strength was further reduced for the specimen heated to 450°F and was 5% less than the code calculated strength.

The experimental results indicate that the accident thermal conditions reduced both the out-of-plane shear strength and stiffness of the tested RC beams It was also confirmed that the concrete contribution to shear stiffness contribution was reduced due to the thermal loading. The code calculated strengths for the specimens with high surface temperature (450°F) resulted in slightly unconservative strength estimates.

In the future studies, the experimental program will be extended to incorporate more parameters including; concrete clear cover, single sided heating, and different heating locations.

REFERENCES

ACI 349-06 (2006). *Code Requirements for Nuclear Safety-Related Concrete Structures and Commentary*. American Concrete Institute, Farmington Hills, MI.

Booth, P.N., Varma, A.H., Sener, K.C., and Malushte, S.R., (2015). *Flexural Behavior and Design of Steel-Plate Composite (SC) Walls for Accident Thermal Loading*. Nuclear Engineering and Design, Special Issue on SMiRT-22 Conference, Vol. 295. Elsevier Science. http://dx.doi.org/10.1016/j.nucengdes.2013.08.035. pp. 231-239.

Yang, Y., Varma, A.H., Kreger, M., and Bradt, T., (2015). *Shear Strength and Behavior of RC Structures with T-Headed Bars for Shear Reinforcement*. Transactions of the 23rd International Conference on Structural Mechanics in Reactor Technology (SMiRT-23), Div-VI: Paper ID# 708, August 10–14, Manchester, UK.